Analytical solutions for the electromagnetic fields of flattened and annular Gaussian laser modes. III. Arbitrary length pulses and spot sizes

Scott M. Sepke and Donald P. Umstadter

Department of Physics and Astronomy, University of Nebraska Lincoln, Nebraska 68588-0111

Received June 26, 2006; accepted July 22, 2006; posted August 8, 2006 (Doc. ID 72334)

In the first two parts of this study, the electromagnetic field components were derived for infinitely long, flattened Gaussian laser beams [J. Opt. Soc. Am. B **23**, 2157 and J. Opt. Soc. Am. B **23**, 2166 (2006)]. These results are now extended without approximation to allow for finite laser pulses having an arbitrary duration beginning with the standard Gaussian beam profile and then generalizing these results to a flattened Gaussian. The resulting models thus allow for all pulse durations and spot sizes from infinite, paraxial beams to single-cycle, wavelength-size spots, with a savings of more than 2 orders of magnitude in computation time. Pulses having fewer than ten cycles exhibit significant modification from the monochromatic fields as a result of the finite bandwidth. Specifically, the energy in the focus is shown to decrease from the theoretical value of 86.5% to as low as 72.2% for a single-cycle pulse. © 2006 Optical Society of America

OCIS codes: 140.7090, 260.2110, 070.2580.

1. INTRODUCTION

Since the advent of chirped pulse amplification, ever shorter laser pulses—approaching the single-cycle limit—have been sought.[1,2] Even a cursory review of the optics literature shows the enormous effort being expended to generate few-cycle fields. Research is ongoing using compression by ionization,[3] Raman scattering,[4,5] filamentation,[6] dielectric reflectors,[7] hollow-core fibers,[8] molecular phase modulation,[9] and even deformable mirrors.[10] Such ultrashort laser pulses find application in many areas of current interest including the acceleration of high-energy monoenergetic electrons; high harmonic generation; photoionization; and control of molecular dynamics, vibrational wave packets, and above-threshold ionization as well as in pump–probe experiments observing the evolution of chemical reactions, melting of solids, and electron motion within solids.[11–24]

With few-cycle lasers available and development progressing at a high rate, detailed vector models of the fields are now needed to describe experiments using such pulses. Molecular dynamics in few-cycle pulses, for example, has recently been shown to depend directly on the electric field and not simply on the intensity distribution.[15,25] Additionally, to correctly describe even an intensity-driven process such as near-threshold ionization, the energy distribution within the laser focus must be known accurately, which is dramatically affected by the inclusion of the laser bandwidth.[25,26] The need for accurate and robust field descriptions for all pulse lengths including the relatively small off-polarization field components has also been underscored many times both theoretically and experimentally in laser–plasma and direct laser–electron interactions.[27–33]

Focused laser vector field models have existed for some time beginning with the standard paraxial result.[34] Lax *et al.*,[35] followed quickly by many others,[36–39] derived higher-order nonparaxial corrections to this theory, and finite pulse corrections have also been added to these perturbative expansions through an additional perturbative series.[40,41] For some time a Fourier-transform solution for a monochromatic Gaussian laser beam has also been known. Cicchitelli *et al.*[31] seem to be the first to have reintroduced this to the laser community followed by at least three others.[11,28,42,43] References 11 and 28 also formally show the integral transform solution including a finite pulse duration. Recently, the monochromatic integral transform solution has been evaluated analytically for all laser spot sizes, decreasing the required computation time for each component by 2 orders of magnitude.[44–46] These solutions also allow for a more general flattened Gaussian radial profile of laser intensity in the focal plane instead of only the standard Gaussian of the previous solutions. The finite pulse solution of Refs. 11 and 28 has also been evaluated analytically for Gaussian beams having spot sizes of the order of a few wavelengths, saving an additional 2 orders of magnitude in computation time over numerical evaluation of the integral solution.[26] With these analytical solutions in hand, the stage is set to develop the field components of a laser having a general flattened Gaussian profile for all spot sizes and any pulse duration.

2. BACKGROUND

The focused laser electric field components for a beam propagating along $\hat{\mathbf{z}}$ and linearly polarized in $\hat{\mathbf{x}}$ resulting from the Fourier-transform solution described above are

$$E_x = \frac{E_0}{\epsilon^2}\left[I_1 + \frac{x^2 - y^2}{r^3} I_2 + \frac{y^2}{r^2} I_3\right] e^{i\phi_0},$$

$$E_y = \frac{E_0}{\epsilon^2}\frac{xy}{r^2}\left[\frac{2}{r} I_2 - I_3\right] e^{i\phi_0},$$

$$E_z = \frac{E_0 x}{\epsilon^2 r} I_4 e^{i(\phi_0 - \pi/2)}, \tag{1}$$

and the magnetic field is identical following the transformation $(x,y)\rightarrow(y,x)$. The parameter ϕ_0 is the carrier-envelope phase, $r^2=x^2+y^2$, the terms I_1 to I_4 are known integrals, and the wavenumber $k=\omega/c=2\pi/\lambda$ and waist w define the beam diffraction angle $\epsilon=2/kw$. Since each frequency component of a finite pulse is, in practice, focused by the same optic with a fixed f-number—defined as the ratio of the optic's focal length to its diameter—and from diffraction theory $w=4(f\text{-number})/k$, ϵ is not a function of the laser frequency.

Given a monochromatic field solution, a finite pulse can be constructed by summing many such solutions of varying frequency with the contribution to the total polychromatic field from each frequency component determined by the temporal envelope imposed on the beam. This is, of course, a continuous sum—an integral. More concretely, given a temporal envelope $f(t)$, the relative magnitude of each frequency component ω is given by the Fourier transform of $f(t)\exp(-i\omega_0 t)$ defined as

$$\tilde{f}(\omega-\omega_0) = \frac{1}{2\pi}\int_{-\infty}^{\infty} f(t) e^{i(\omega-\omega_0)t} \mathrm{d}t,$$

where ω_0 is the laser carrier frequency. The field integrals I_1 to I_4 in Eqs. (1) for a pulse having temporal envelope $f(t)$ can then be written formally as

$$I_1 = \int_{-\infty}^{\infty} \tilde{f}(\omega-\omega_0) e^{-i\omega t} \int_0^1 e^{\mu}(m+m^2) J_0(\Lambda) \mathrm{d}m \mathrm{d}\omega,$$

$$I_2 = \int_{-\infty}^{\infty} \tilde{f}(\omega-\omega_0) \frac{e^{-i\omega t}}{k} \int_0^1 e^{\mu} J_1(\Lambda) \sqrt{1-m^2} \mathrm{d}m \mathrm{d}\omega,$$

$$I_3 = \int_{-\infty}^{\infty} \tilde{f}(\omega-\omega_0) e^{-i\omega t} \int_0^1 e^{\mu} J_0(\Lambda) (1-m^2) \mathrm{d}m \mathrm{d}\omega,$$

$$I_4 = \int_{-\infty}^{\infty} \tilde{f}(\omega-\omega_0) e^{-i\omega t} \int_0^1 e^{\mu} \kappa(m) J_1(\Lambda) \mathrm{d}m \mathrm{d}\omega, \tag{2}$$

where the inner integration is the standard infinite beam solution for a Gaussian intensity profile, $\Lambda=kr\sqrt{1-m^2}$, $\mu=ikzm+(m^2-1)/\epsilon^2$, and $\kappa(m)=(1+m)\sqrt{1-m^2}$.

In this paper, beginning with the monochromatic solutions of Parts I and II of this study, the electromagnetic field components for a general flattened Gaussian laser profile are derived allowing now for an arbitrary pulse duration.[45,46] First, in Subsections 3.A and 3.B, a tightly focused (i.e., $w_0\sim\lambda_0$) Gaussian beam with a cosine-squared pulse envelope is derived and some important limits are explored. In Subsection 3.C this is extended to allow for the more general flattened Gaussian beam profile. In Section 4, Eqs. (1) and (2) are solved assuming a large focal spot (i.e., $w_0\gg\lambda_0$) and a Gaussian temporal envelope: first, for a Gaussian beam and then for a flattened Gaussian. In Section 5 we discuss the effect of including a finite laser bandwidth on the beam itself. As the pulse duration decreases below ten cycles—roughly 27 fs for a Ti:sapphire pulse, for example—the laser fields begin to exhibit significant alteration relative to monochromatic fields. An important change in the character of the fields occurs in the fraction of the laser energy in the focus. For an infinite-duration Gaussian beam, this is equal to $1-\exp(-2)\approx 86.47\%$. For pulses having fewer than five cycles, this fraction drops precipitously, decreasing to as low as 72.26% for a single-cycle pulse. Comments are also made regarding the stability of this model at all times and positions and the more than 2 orders-of-magnitude savings in computation time afforded by this technique.

The fields derived in this paper completely characterize the vector nature of any diffraction-limited laser whose focal-plane profile can be described as $f(r^2)\exp(-r^2/w_0^2)$ for any well-behaved $f(r^2)$ focused to an arbitrary spot size w_0 and having any pulse duration even down to a single cycle. Of course, these models can also be used to describe the scalar properties of such laser pulses as well since $I=U^2\propto[|\mathbf{E}|^2+|\mathbf{B}|^2]$.

3. LARGE-NUMERICAL-APERTURE FOCUSING

A. Gaussian Intensity Profile

In Part I of this study,[45] the monochromatic functions I_n are computed for a beam having a nominally Gaussian focal-plane distribution expressed as $E_x(z=0)=B_y(z=0)=E_0\exp(-r^2/w_0^2)$, giving the result

$$I_1 = 2e^{-i\omega_0 t}\sum_{s=0}^{\infty} \hat{a}_{s,0} i^s C_s^{1/2}\left(\frac{z}{\rho}\right) j_s(\omega\bar{\rho}), \tag{3}$$

$$I_2 = -\frac{2c^2}{\omega_0^2} e^{-i\omega_0 t}\sum_{s=0}^{\infty} \tilde{b}_{s,0} i^s \partial_r\left[C_s^{1/2}\left(\frac{z}{\rho}\right) j_s(\omega\bar{\rho})\right], \tag{4}$$

$$I_3 = 2e^{-i\omega_0 t}\sum_{s=0}^{\infty} \hat{c}_{s,0} i^s C_s^{1/2}\left(\frac{z}{\rho}\right) j_s(\omega\bar{\rho}), \tag{5}$$

$$I_4 = i\frac{2c}{\omega_0} e^{-i\omega_0 t}\sum_{s=0}^{\infty} \hat{d}_{s,0} i^s \partial_r\left[C_s^{1/2}\left(\frac{z}{\rho}\right) j_s(\omega\bar{\rho})\right], \tag{6}$$

where $\partial_r(\cdot)$ is the derivative with respect to r; $C_s^{\lambda}(x)$ are the Gegenbauer polynomials; $j_s(x)$ are the spherical Bessel functions of the first kind; $\rho^2=r^2+z^2$; $\bar{\rho}=\rho/c$; and $\hat{a}_{s,0}$, $\hat{b}_{s,0}$, $\hat{c}_{s,0}$ and $\hat{d}_{s,0}$ are given by the recursion

$$\hat{b}_{0,d} = \frac{1}{4}(-i\epsilon)^{d+1}\gamma\left(\frac{d+1}{2}, -\frac{1}{\epsilon^2}\right) e^{-(1/\epsilon^2)},$$

$$\hat{b}_{1,d} = 3\hat{b}_{0,d+1},$$

$$\hat{b}_{s,d} = \left(\frac{2s-1}{s}\right)\left[\hat{b}_{s-1,d+1} - \left(\frac{s-1}{2s-3}\right)\hat{b}_{s-2,d}\right],$$

where $\gamma(n,x)$ is the lower incomplete gamma function, and[45,47]

$$\hat{a}_{s,d} = \hat{b}_{s,d+1} + \hat{b}_{s,d+2},$$

$$\hat{c}_{s,d} = \hat{b}_{s,d} - \hat{b}_{s,d+2},$$

$$\hat{d}_{s,d} = \hat{b}_{s,d} + \hat{b}_{s,d+1}. \tag{7}$$

As each of these parameters is only a function of the diffraction angle ϵ, the only frequency dependence present in these four expressions [Eqs. (3)–(6)] is of the form $\omega^{-n} j_s(\omega\bar{\rho})$ for $n=0,1,2$. Thus, to evaluate the finite pulse integrals of Eqs. (2) and generate the polychromatic fields, only the three integrals

$$\mathcal{I}_{s,n} = 2i^s \int_{-\infty}^{\infty} \tilde{f}(\omega-\omega_0) e^{-i(\omega-\omega_0)t} \omega^{-n} j_s(\omega\bar{\rho}) \mathrm{d}\omega$$

need to be evaluated for all nonnegative integers s and $n=0,1,2$. The polychromatic electric—and hence magnetic field—components are still given formally by Eqs. (1), and the functions I_1–I_4 are defined according to Eqs. (2) to account for the laser bandwidth as

$$I_1 = e^{-i\omega_0 t} \sum_{s=0}^{\infty} \hat{a}_{s,0} C_s^{1/2}\left(\frac{z}{\rho}\right) \mathcal{I}_{s,0}, \tag{8}$$

$$I_2 = \frac{cr}{\rho} e^{-i\omega_0 t} \sum_{s=0}^{\infty} \hat{b}_{s,0} \left\{ \left(\frac{cz}{\rho^2}\right) C_{s-1}^{3/2}\left(\frac{z}{\rho}\right) \mathcal{I}_{s,2} - iC_s^{1/2}\left(\frac{z}{\rho}\right) \times \left[\frac{s\mathcal{I}_{s-1,1} + (s+1)\mathcal{I}_{s+1,1}}{2s+1} \right] \right\}, \tag{9}$$

$$I_3 = e^{-i\omega_0 t} \sum_{s=0}^{\infty} \hat{c}_{s,0} C_s^{1/2}\left(\frac{z}{\rho}\right) \mathcal{I}_{s,0}, \tag{10}$$

$$I_4 = -\frac{r}{\rho} e^{-i\omega_0 t} \sum_{s=0}^{\infty} \hat{d}_{s,0} \left\{ \left(i\frac{cz}{\rho^2}\right) C_{s-1}^{3/2}\left(\frac{z}{\rho}\right) \mathcal{I}_{s,1} + C_s^{1/2}\left(\frac{z}{\rho}\right) \times \left[\frac{s\mathcal{I}_{s-1,0} + (s+1)\mathcal{I}_{s+1,0}}{2s+1} \right] \right\}, \tag{11}$$

taking $s\mathcal{I}_{s-1,0} \equiv 0$ when $s=0$.

For an infinitely long beam, $f(t)\equiv 1$ and $\tilde{f}(\omega-\omega_0)=\delta(\omega-\omega_0)$ where $\delta(x)$ is the Dirac delta function, and the monochromatic solution of Eqs. (3)–(6) is recovered. For more complicated envelopes such as a cosine-squared pulse, $f(t)=\cos^2(\pi t/2\Delta\tau)$, the integrals $\mathcal{I}_{s,n}$ become difficult to evaluate directly. They can, however, also be cast in the time domain by making use of the convolution theorem giving[48]

$$\mathcal{I}_{s,n} = \frac{i^s}{\pi} \int_{-\infty}^{\infty} f(t-T) H_n(T) e^{i\omega_0 T} \mathrm{d}T, \tag{12}$$

where $f(t-T)$ is the temporal envelope translated by T and $H_n(T)$ is the inverse Fourier transform of $\omega^{-n} j_s(\omega\bar{\rho})$:

$$H_n(T) = \int_{-\infty}^{\infty} j_s(\omega\bar{\rho}) \omega^{-n} e^{-i\omega T} \mathrm{d}\omega, \tag{13}$$

which can be evaluated exactly.

The function $H_0(T)$ has been worked out by Ludu and O'Connell and is simply the inverse Fourier transform of the spherical Bessel function of the first kind[49]:

$$H_0(T) = \pi i^s \,\mathrm{rect}\left(\frac{T}{\bar{\rho}}\right) \sum_{k=0}^{2k\leqslant s} C_k^{(s)} (-1)^k \bar{\rho}^{2k-s-1} T^{s-2k},$$

where $\mathrm{rect}(T/\bar{\rho})=[\mathcal{H}(T+\bar{\rho})-\mathcal{H}(T-\bar{\rho})]$, $\mathcal{H}(x)$ is the Heaviside step function that is zero for $x<0$ and one for $x>0$, and the constants $C_k^{(s)}$ are given by the recursion

$$(l+1)C_k^{(l+1)} = lC_{k-1}^{(l-1)} - (2l+1)C_k^{(l)}$$

for $C_0^{(0)}=1$, $C_1^{(2)}=1/2$, and $C_k^{(s)}=0$ for all $(s,k)<0$.

From Eq. (13) the transforms $H_1(T)$ and $H_2(T)$ can be related to $H_0(T)$ through the equations

$$\frac{\mathrm{d}H_1}{\mathrm{d}T} = -iH_0(T), \quad \frac{\mathrm{d}^2 H_2}{\mathrm{d}T^2} = -H_0(T).$$

Solving each of these ordinary differential equations by separation of variables first gives the transform $H_1(T)$:

$$H_1(T) = \frac{\pi}{i^{1-s}} \sum_{k=0}^{2k\leqslant s} \left[\frac{C_k^{(s)}(-1)^k}{s-2k+1} \right] \left\{ \left(\frac{T}{\bar{\rho}}\right)^{s-2k+1} \mathrm{rect}\left(\frac{T}{\bar{\rho}}\right) + (-1)^{s-2k}[\mathcal{H}(T+\bar{\rho}) + (-1)^{s-2k}\mathcal{H}(T-\bar{\rho})] \right\},$$

and then the function $H_2(T)$ follows from one additional integration as

$$H_2(T) = -\pi i^s \sum_{k=0}^{2k\leqslant s} C_k^{(s)}(-1)^k \times \left\{ \frac{\bar{\rho}}{(s-2k+1)(s-2k+2)} \mathrm{rect}\left(\frac{T}{\bar{\rho}}\right) \left(\frac{T}{\bar{\rho}}\right)^{s-2k+2} + \frac{\bar{\rho}(-1)^{s-2k}}{s-2k+2} [\mathcal{H}(T+\bar{\rho}) - (-1)^{s-2k}\mathcal{H}(T-\bar{\rho})] + \frac{(-1)^{s-2k}}{s-2k+1} [\mathcal{H}(T+\bar{\rho}) + (-1)^{s-2k}\mathcal{H}(T-\bar{\rho})]T \right\},$$

completing the specification of the time-domain form of $\mathcal{I}_{s,n}$ of Eq. (12).

For a cosine-squared temporal envelope as described above, each of the integrals $\mathcal{I}_{s,n}$ are readily evaluated in the time domain as shown in Ref. 26 giving

$$\mathcal{I}_{s,0} = \sum_{k=0}^{2k\leqslant s} C_k^{(s)}(-1)^{s+k} \bar{\rho}^{2k-s-1} \mathcal{F}_{s-2k}(-\bar{\rho},\bar{\rho}),$$

$$\mathcal{I}_{s,1} = -i \sum_{k=0}^{2k\leqslant s} \frac{C_k^{(s)}(-1)^{s+k}}{s-2k+1} \left(\frac{\mathcal{F}_{s-2k+1}(-\bar{\rho},\bar{\rho})}{\bar{\rho}^{s-2k+1}} + (-1)^{s-2k}\{\mathcal{F}_0(-\bar{\rho},\rho) + [1+(-1)^{s-2k}]\mathcal{F}_0(\bar{\rho},\infty)\} \right),$$

$$\mathcal{I}_{s,2} = -\sum_{k=0}^{2k\leqslant s} C_k^{(s)}(-1)^{s+k}\left(\frac{\mathcal{F}_{s-2k+2}(-\bar{\rho},\bar{\rho})\bar{\rho}^{2k-s-1}}{(s-2k+1)(s-2k+2)}\right.$$
$$+\frac{\bar{\rho}(-1)^{s-2k}}{s-2k+2}\{\mathcal{F}_0(-\bar{\rho},\bar{\rho})$$
$$+[1-(-1)^{s-2k}]\mathcal{F}_0(\bar{\rho},\infty)\}+\frac{(-1)^{s-2k}}{s-2k+1}\{\mathcal{F}_1(-\bar{\rho},\bar{\rho})$$
$$\left.+[1+(-1)^{s-2k}]\mathcal{F}_1(\bar{\rho},\infty)\}\right),$$

where the functions $\mathcal{F}_n(\alpha,\beta)$ are defined as

$$\mathcal{F}_n(\alpha,\beta)=\frac{1}{4}\{(2\mathcal{C}_n(\omega_0)+\cos(\Omega_0 t)[\mathcal{C}_n(\Omega_+)+\mathcal{C}_n(\Omega_-)]+\sin(\Omega_0 t)$$
$$\times[\mathcal{S}_n(\Omega_+)+\mathcal{S}_n(\Omega_-)])+i(2\mathcal{S}_n(\omega_0)+\cos(\Omega_0 t)$$
$$\times[\mathcal{S}_n(\Omega_+)-\mathcal{S}_n(\Omega_-)]-\sin(\Omega_0 t)[\mathcal{C}_n(\Omega_+)$$
$$-\mathcal{C}_n(\Omega_-)])\}|_\alpha^\beta,$$

for $\Omega_0=\pi/\Delta\tau$ and $\Omega_\pm=\Omega_0\pm\omega_0$. The limits α and β are those formally imposed by the Heaviside functions. As the cosine-squared envelope is only nonzero in a finite region, the true bounds of this integration are the intersection of these regions: $T\in\{[\alpha,\beta]\cap[t-\Delta\tau,t+\Delta\tau]\}$. Finally, to complete this solution, define the functions $\mathcal{S}_p(\omega)$ and $\mathcal{C}_p(\omega)$ as the well-known integrals

$$\mathcal{S}_p(\omega)\equiv\int x^p\sin(\omega x)\mathrm{d}x$$
$$=(-1)^{p/2+1}(p!)\left[\cos(\omega x)\sum_{k=0}^{p/2}\frac{(-1)^k x^{2k}}{(2k)!\omega^{p-2k+1}}\right.$$
$$\left.+\sin(\omega x)\sum_{k=1}^{p/2}\frac{(-1)^{k+1}x^{2k-1}}{(2k-1)!\omega^{p-2k+2}}\right],\quad p\text{ even},$$
$$=-\left(\frac{x^p}{\omega}\right)\cos(\omega x)+\left(\frac{p}{\omega}\right)\mathcal{C}_{p-1}(\omega),\quad p\text{ odd},$$

$$\mathcal{C}_p(\omega)\equiv\int x^p\cos(\omega x)\mathrm{d}x$$
$$=(-1)^{p/2}(p!)\left[\sin(\omega x)\sum_{k=0}^{p/2}\frac{(-1)^k x^{2k}}{(2k)!\omega^{p-2k+1}}\right.$$
$$\left.-\cos(\omega x)\sum_{k=1}^{p/2}\frac{(-1)^{k+1}x^{2k-1}}{(2k-1)!\omega^{p-2k+2}}\right],\quad p\text{ even}$$
$$=\left(\frac{x^p}{\omega}\right)\sin(\omega x)-\left(\frac{p}{\omega}\right)\mathcal{S}_{p-1}(\omega),\quad p\text{ odd}$$

for all nonnegative integers p.

B. Some Important Limits

To complete this model, the limits as r and ρ go to zero must be computed. In Part I, these limits were shown for the monochromatic fields to be[45]

$$\lim_{r\to 0}E_x=\frac{E_0}{\epsilon^2}\sum_{s=0}^{\infty}(2\hat{a}_{s,0}+\hat{c}_{s,0})j_s(k_0 z)i^s e^{-i(\omega_0 t-\phi_0)},$$

$$\lim_{\rho\to 0}E_x=\frac{E_0}{\epsilon^2}(2\hat{a}_{0,0}+\hat{c}_{0,0})e^{-i(\omega_0 t-\phi_0)},\tag{14}$$

with $E_y=E_z\equiv 0$. Fourier transforming the limit as r approaches 0 according to Eqs. (2) is, of course, equivalent to simply replacing $2i^s j_s(kz)$ with $\mathcal{I}_{s,0}$, meaning that as r approaches zero,

$$\lim_{r\to 0}E_x=\left.\frac{E_0}{2\epsilon^2}e^{-i(\omega_0 t-\phi_0)}\sum_{s=0}^{\infty}(2\hat{a}_{s,0}+\hat{c}_{s,0})\mathcal{I}_{s,0}\right|_{r=0},$$

and again, $E_y=E_z\equiv 0$. In the limit that ρ approaches zero,

$$\lim_{\rho\to 0}\mathcal{I}_{s,0}=\sum_{k=0}^{2k\leqslant s}C_k^{(s)}(-1)^{s+k}\left[\frac{T_1^{s-2k+1}-T_0^{s-2k+1}}{s-2k+1}\right]f(t),$$

where $f(t)$ is the temporal envelope, a cosine-squared function is this case. This integration has been carried out formally over the range $T\in[T_0,T_1]$, which is the intersection of the ranges $[-\bar{\rho},\bar{\rho}]$ and $[t-\Delta\tau,t+\Delta\tau]$. E_x is then, as $\rho\to 0$,

$$\lim_{\rho\to 0}E_x=\frac{E_0}{\epsilon^2}e^{-i(\omega_0 t-\phi_0)}\cos^2\left(\frac{\pi t}{2\Delta\tau}\right)(2\hat{a}_{0,0}+\hat{c}_{0,0})$$
$$\times\sum_{k=0}^{2k\leqslant s}C_k^{(s)}(-1)^{s+k}\left[\frac{T_1^{s-2k+1}-T_0^{s-2k+1}}{s-2k+1}\right].$$

In the limit of a long laser pulse, $\mathcal{I}_{s,0}$ reduces to

$$\lim_{\rho\to 0}\mathcal{I}_{s,0}=2\cos^2\left(\frac{\pi t}{2\Delta\tau}\right)$$

for $s=0$ and zero for all other s. Thus the monochromatic value of Eqs. (14) is, in fact, recovered, and the electric and magnetic fields are now fully specified in all time and space for a Gaussian laser profile.

C. General Flattened Gaussian Profile

Following again the model of Refs. 44 and 45, this result can be easily extended to allow for flattened and annular Gaussian transverse profiles—i.e., for $E_x(z=0)$ and $B_y(z=0)$ taking the form

$$E_0\sum_{N=0}^{\infty}A_N\left(\frac{r}{w_0}\right)^{2N}\exp\left(-\frac{r^2}{w_0^2}\right),$$

where A_N are arbitrary complex-valued fitting parameters—by simply replacing E_0 with $E_0\Sigma_{N=0}^{\infty}A_N N!$ and $\hat{b}_{s,n}$ with

$$\hat{b}_{s,n}^N=\sum_{\nu=0}^{N}\sum_{k=0}^{\nu}(-1)^k\epsilon^{-2\nu}\left[\frac{N!\hat{b}_{s,2\nu-2k+n}}{(N-\nu)!\nu!(\nu-k)!k!}\right],$$

in Eqs. (1) and (7)–(11).[44,45]

4. SMALL-NUMERICAL-APERTURE FOCUSING

A. Gaussian Intensity Profile

A similar calculation can be carried out for loosely focused beams ($w_0 \gg \lambda_0$) beginning from the spherical Hankel field model derived in Part II of this study.[46] Recall that the symmetric electric field components for a Gaussian profile are given by

$$E_x = -iE_0 \sum_{n=0}^{\infty} \epsilon^{2n} \left(\frac{k_0 z}{2}\right)^{n+1} h_n^{(1)}(k_0 z) \partial_y^2 G_n\left(\frac{r^2}{w_0^2}\right) + \frac{E_0}{2} \sum_{n=0}^{\infty} \epsilon^{2n} \left(\frac{k_0 z}{2}\right)^{n} F_x(k_0 z) G_n\left(\frac{r^2}{w_0^2}\right),$$

$$E_y = iE_0 \sum_{n=0}^{\infty} \epsilon^{2n} \left(\frac{k_0 z}{2}\right)^{n+1} h_n^{(1)}(k_0 z) \partial_{xy}^2 G_n\left(\frac{r^2}{w_0^2}\right),$$

$$E_z = E_0 \sum_{n=0}^{\infty} \epsilon^{2n} \left(\frac{k_0 z}{2}\right)^{n+1} F_z(k_0 z) \partial_x G_n\left(\frac{r^2}{w_0^2}\right),$$

where $F_x(z) \equiv [(z-2in)h_{n-1}^{(1)}(z) + izh_n^{(1)}(z)]$, $F_z(z) \equiv [ih_{n-1}^{(1)}(z) - h_n^{(1)}(z)]$, $h_n^{(1)}(z)$ are the spherical Hankel functions of the first kind, $G_n(\xi) = \exp(-i[\omega_0 t - \phi_0] - \xi) L_n^0(\xi)$ where $L_n^k(\xi)$ are the kth associated Laguerre polynomials of order n, ϕ_0 is the carrier-envelope phase, and again the magnetic field is identical following the transformation $(x,y) \to (y,x)$.

These field components can be rewritten collecting powers of ω as shown in Table 1. The functions $\mathcal{L}_{n,m}^k$ then contain all of the frequency dependence of the fields. For an infinite beam containing only the carrier frequency ω_0, these functions are simply

Table 1. Electric Field Components for a Loosely Focused Gaussian Beam[a]

$$E_x = E_0 e^{i\phi_0} \Bigg\{ \mathcal{L}_{0,0}^0 + \Sigma_{n=1}^{\infty} \epsilon^{2n} \Bigg[\Sigma_{k=0}^{n} \Gamma_{n,k} i^{-n-k} \left(\frac{z}{c}\right)^{n-k} \mathcal{L}_{n,n-k}^0 + \epsilon^2 \Sigma_{k=0}^{n} \Gamma_{n,k} i^{-n-k} \left(\frac{z}{c}\right)^{n-k} \left\{ \mathcal{Z}_{n-k} - \left(\frac{y^2 \epsilon^2}{2c^2}\right) \mathcal{Y}_{n-k+2} \right\} + n \Sigma_{k=0}^{n-1} \Gamma_{n-1,k} i^{-n-k-1} \left(\frac{z}{c}\right)^{n-k-1} \mathcal{L}_{n,n-k-1}^0 + \frac{1}{2} \Sigma_{k=0}^{n-1} \Gamma_{n-1,k} i^{-n-k} \left(\frac{z}{c}\right)^{n-k} \mathcal{L}_{n,n-k}^0 \Bigg] \Bigg\}.$$

$$E_y = E_0 e^{i\phi_0} \frac{xy\epsilon^4}{4c^2} \Sigma_{n=0}^{\infty} \epsilon^{2n} \Sigma_{k=0}^{n} \Gamma_{n,k} i^{-n-k} \left(\frac{z}{c}\right)^{n-k} \mathcal{Y}_{n-k+2}.$$

$$E_z = -iE_0 e^{i\phi_0} \left(\frac{x\epsilon^2}{2c}\right) \Bigg\{ \mathcal{L}_{0,1}^0 + \Sigma_{n=1}^{\infty} \epsilon^{2n} \frac{(2n)!}{n! 2^{2n+1}} \mathcal{Z}_1 + \Sigma_{n=1}^{\infty} \epsilon^{2n} \Sigma_{k=0}^{n-1} \left(\frac{1}{2} \Gamma_{n-1,k} + \Gamma_{n,k}\right) i^{-n-k} \left(\frac{z}{c}\right)^{n-k} \mathcal{Z}_{n-k+1} \Bigg\}.$$

[a] The magnetic field is identical under the rotation $(x,y) \to (y,x)$. The functions $\mathcal{Y}_M \equiv [\mathcal{L}_{n,M}^0 + 2\mathcal{L}_{n-1,M}^1 + \mathcal{L}_{n-2,M}^2]$ and $\mathcal{Z}_M \equiv [\mathcal{L}_{n,M}^0 + \mathcal{L}_{n-1,M}^1]$, and the parameter $\Gamma_{n,k} = (-1)^k [(n+k)!/k!(n-k)!2^{n+k+1}]$ for all nonnegative integers n and k.

$$\mathcal{L}_{n,m}^k \equiv e^{-i\omega_0(t-z/c)} e^{-r^2/w_0^2} \omega_0^m L_n^k\left(\frac{r^2}{w_0^2}\right).$$

To include a finite pulse, each of these field components must be Fourier transformed as in Eqs. (2). Letting the temporal envelope $f(t) = \exp(-[t-z/c]^2/\Delta\tau^2)$, the fields remain formally the same, but now the functions $\mathcal{L}_{n,m}^k$ take on the definition

$$\mathcal{L}_{n,m}^k \equiv \sum_{\nu=0}^{n} \frac{(-1)^\nu}{\nu!} \binom{n+k}{\nu+k} \left(\frac{r\epsilon}{2c}\right)^{2\nu} \kappa_{2\nu+m},$$

where the parameters κ_n are

$$\kappa_n = \int_{-\infty}^{\infty} \tilde{f}(\omega - \omega_0) e^{-i\omega(t-z/c)} e^{-r^2\epsilon^2\omega^2/4c^2} \omega^n \mathrm{d}\omega = \left(\frac{\omega_0^n}{2\sqrt{\pi}}\right) \exp\left(\frac{\omega_0^2 \Delta\tau^2}{4}[\delta - 1] - \frac{\delta\eta^2}{\omega_0^2 \Delta\tau^2}\right) e^{-i\delta\eta} \times \sum_{k=0}^{n} \sum_{m=0}^{n-k} \gamma_{n,k,m} \frac{\delta^{n-k/2+1/2} \eta^m}{(\omega_0 \Delta\tau)^{2m+k}},$$

for $\eta = \omega_0 t - k_0 z$, $\delta = [1 + (r\epsilon/c\Delta\tau)^2]^{-1}$, and

$$\gamma_{n,k,m} = \frac{n! 2^{k+m} \Gamma\left(\frac{k+1}{2}\right)[1 + (-1)^k]}{i^m (n-k-m)! k! m!}$$

for nonnegative integers n, k, and m.

The effect of the polychromatic corrections and the link between spatial and temporal bandwidth are characterized by the parameter δ, and interestingly, this coupling is tied to the radial coordinate r. As expected, when the spot size w_0 becomes arbitrarily large and $\epsilon \to 0$, this solution correctly reduces to the plane-wave case:

$$E_x \to E_0 e^{-i(\eta - \phi_0)} \exp\left[\frac{(t - z/c)^2}{\Delta\tau^2}\right],$$

and $E_y \equiv E_z \equiv 0$. Also, as the pulse duration becomes large, $\delta \to 1$ and the monochromatic result is recovered.

B. General Flattened Gaussian Profile

The loose focusing model given in Table 1 can be easily extended to allow for a general flattened Gaussian transverse profile as well. As with the similar conversion in the tightly focused case, the amplitude E_0 is formally replaced by $E_0 \Sigma_{N=0}^{\infty} A_N N!$. To complete the generalization, the definition of $\mathcal{L}_{n,m}^k$ must also be modified so that $\mathcal{L}_{n,m}^k$ is replaced by

$$\mathcal{L}_{n,m}^{k,N} \equiv \sum_{l=0}^{N} \Delta_{ln}^N \sum_{\nu=0}^{n+l} \frac{(-1)^\nu}{\nu!} \binom{n+l+k}{\nu+k} \left(\frac{r\epsilon}{2c}\right)^{2\nu} \kappa_{2\nu+m},$$

where the parameter Δ_{ln}^N is

$$\Delta_{ln}^N \equiv (-1)^l \left[\frac{N!(l+n)!}{(N-l)! n! l! l!}\right],$$

which is $2^{n+1}/N!$ times the Δ_{ln}^N defined in Part II.[46]

5. RESULTS AND DISCUSSION

Figure 1 shows the fraction of the laser energy within the nominal waist w_0 at the peak of the pulse as a function of the laser-pulse duration for a Gaussian laser profile: that is, $A_0=1$ and $A_{N>0}=0$. For an infinite beam, this value is equal to $1-\exp(-2)\approx 0.86466$, and this is shown as the solid line for reference. For pulses containing more than ten cycles full width at half-maximum (FWHM) and focused to spot sizes larger than $3/2\lambda_0$, this limit is met. This is illustrated explicitly in Fig. 1 for $w_0=10\lambda_0$. As the pulse length drops below ten cycles, the range of frequencies and the corresponding range of focused spot sizes associated with the pulse tend to increase the breadth of the radial distribution of energy in the focal plane. This results in a concomitant decrease in the fraction of the total energy in the focus. This decrease is observed for all spot sizes and becomes pronounced as the pulse duration drops below five cycles.

Figure 1 also shows another interesting effect, this time resulting from the non-Gaussian shape of the laser intensity profile for tightly focused beams, that is, for $w_0 \lesssim 3/2\lambda_0$. Recall from Part I of this study that for monochromatic pulses, the amplitude of the laser at the focus—i.e., at $(x,y,z)=(0,0,0)$—is not, in general, equal to E_0 but is instead given by[45]

$$\lim_{\rho\to 0}\frac{E_x}{E_0}=\frac{1}{4}(3-2e^{-1/\epsilon^2})-i\left(\frac{2-\epsilon^2}{8\epsilon}\right)e^{-1/\epsilon^2}\gamma\left(\frac{1}{2},-\frac{1}{\epsilon^2}\right).$$

This results because of the non-Gaussian terms added to the nominally Gaussian E_x and B_y when the solution is symmetrized. For $w_0<3/5\lambda_0$, these terms tend to decrease the peak amplitude of the beam by adding flattop terms to the field, thereby effectively widening the focal spot of the laser. This is exhibited in Fig. 1 for $w_0=1/2\lambda_0$ plotted as the blue circles. In that case, the long pulse limit of the fraction of energy contained within $r\leqslant w_0$ is less than the Gaussian value. Conversely, for laser spot sizes between $3/5\lambda_0$ and $3/2\lambda_0$, $\lim_{\rho\to 0}(E_x/E_0)\gtrsim 1$, and hence, the non-Gaussian terms added by the symmetrization now tend to concentrate the energy preferentially within the nominal spot. Thus, the long pulse limit of the fraction of energy in the waist is now greater than the purely Gaussian value. This is clearly shown in Fig. 1 for the case of $f-1$ focusing, which results in a spot size $w_0=(2/\pi)\lambda_0$.

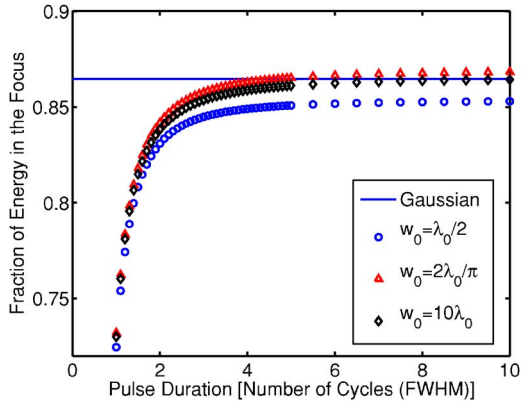

Fig. 1. (Color online) Fraction of the total energy in the focus at the peak of the pulse as a function of the pulse duration for $w_0=\lambda_0/2$ (blue circles), $w_0=(2/\pi)\lambda_0$ (red triangles), and $w_0=10\lambda_0$ (black diamonds). The limit of a perfect Gaussian $[1-\exp(-2)\approx 0.86466]$ is included as the blue line for reference.

Within the range of validity of each of the field models derived here, each of the field components is stable for all values of time and space. For the tightly focused model, $\sim 20(1+N/2)(w/\lambda_0)$ terms are required for the Fourier–Gegenbauer expansion to converge. Comparing this solution with a numerical integration of the frequency transforms shows a decrease in the computation time of 2 orders of magnitude. Specifically, the time decreases by a factor of ~ 675 when the fields are calculated at 400 points evenly spaced in the focal plane when we evaluate the integrals using a Romberg solver.

The spherical Hankel expansion used to model loosely focused pulses requires only one or two series terms even for focusing down to a few wavelengths in the focal plane, that is, when $z=0$. As described in detail in Part II, however, the larger that value of z, the more terms are required for the series to converge.[46] Again, comparing field calculations, a roughly 2 orders-of-magnitude improvement is obtained over evaluating the frequency transforms directly, depending on how many series terms are required.

6. CONCLUSION

In this paper, the six electromagnetic field components of a focused laser pulse have been derived allowing for any spot size, pulse duration, and intensity profile of the form $f(r^2)\exp(-r^2/w_0^2)$. This includes as the simplest example the classic Gaussian laser profile, which has been derived in integral form several times. The analytic forms developed in this study improve the computation time of the field components by more than 2 orders of magnitude for a monochromatic beam and an additional 2 orders are gained over the integral form for a finite pulse.[26,44–46]

These solutions are well suited to large-scale numerical calculation. In addition to the time savings noted above, save for the expansion coefficients $\hat{b}_{s,d}$ that need only be tabulated once *a priori* for a given spot size in the tightly focused Fourier–Gegenbauer model, the fields derived here are built from only standard functions available on any computing platform: sines, cosines, exponentials, and polynomials. The formal structure of these fields is also dominated by nested sums that are easily amenable to numerical calculation both in small numerical solvers that model such things as above-threshold ionization or classical molecular dynamics and large-scale simulations such as plasma fluid and particle-in-cell codes. Modeling of a host of physical phenomena can now include not only simple plane-wave laser fields but also the true focused character of the realistic laser pulses used in experiments.

ACKNOWLEDGMENTS

The authors gratefully acknowledge support for this work from the National Science Foundation and from the Chemical Sciences, Geosciences, and Biosciences Division

of the Office of Basic Energy Sciences, U.S. Department of Energy. S. Sepke thanks Todd Sepke for many helpful and insightful discussions.

The e-mail address for S. M. Sepke is ssepke2@unlserve.unl.edu.

REFERENCES

1. M. Nisoli, S. DeSilvestri, O. Svelto, R. Szipcs, K. Ferencz, C. Spielmann, S. Sartania, and F. Krausz, "Compression of high-energy laser pulses below 5 fs," Opt. Lett. **22**, 522–524 (1997).
2. J. Seres, A. Müller, E. Seres, K. O'Keeffe, M. Lenner, R. Herzog, D. Kaplan, C. Spielmann, and F. Krausz, "Sub-10 -fs, terawatt-scale Ti:sapphire laser system," Opt. Lett. **28**, 1832–1834 (2003).
3. N. L. Wagner, E. A. Gibson, T. Popmintchev, and I. P. Christov, "Self-compression of ultrashort pulses through ionization-induced spatiotemproal reshaping," Phys. Rev. Lett. **93**, 173902 (2004).
4. A. A. Balakin, G. M. Fraiman, N. J. Fisch, and S. Suckewer, "Backward Raman amplification in a partially ionized gas," Phys. Rev. E **72**, 036401 (2005).
5. V. P. Kalosha and J. Herrmann, "Ultrawide spectral broadening and compression of single extremely short pulses in the visible, uv-vuv, and middle infrared by high-order stimulated Raman scattering," Phys. Rev. A **68**, 023812 (2003).
6. A. Couairon, M. Franco, A. Mysyrowicz, J. Biegert, and U. Keller, "Pulse self-compression to the single-cycle limit by filamentation in a gas with a pressure gradient," Opt. Lett. **30**, 2657–2659 (2005).
7. A. J. Waddie, M. J. Thomson, and M. R. Taghizadeh, "Comparison of one- and two-dimensional dielectric reflector geometries for high-energy laser pulse compression," Opt. Lett. **30**, 991–993 (2005).
8. M. Spanner, M. Y. Ivanov, V. Kalosha, J. Hermann, D. A. Wiersma, and M. Pshenichnikov, "Tunable optimal compression of ultrabroadband pulses by cross-phase modulation," Opt. Lett. **28**, 749–751 (2003).
9. N. Zhavoronkov and G. Korn, "Generation of single intense short optical pulses by ultrafast molecular phase modulation," Phys. Rev. Lett. **88**, 203901 (2002).
10. E. Zeek, K. Maginnis, S. Backus, U. Russek, M. Murnane, G. Mourou, H. Kapteyn, and G. Vdovin, "Pulse compression by use of deformable mirrors," Opt. Lett. **24**, 493–495 (1999).
11. B. Rau, T. Tajima, and H. Hojo, "Coherent electron acceleration by subcycle laser pulses," Phys. Rev. Lett. **78**, 3310–3313 (1997).
12. J. Faure, Y. Glinec, J. J. Santos, F. Ewald, J.-P. Rousseau, S. Kiselev, A. Pukhov, T. Hosokai, and V. Malka, "Observation of laser-pulse shortening in nonlinear plasma waves," Phys. Rev. Lett. **95**, 205003 (2005).
13. N. M. Naumova, J. A. Nees, I. V. Sokolov, B. Houl, and G. A. Mourou, "Relativistic generation of isolated attosecond pulses in a lambda-cubed focal volume," Phys. Rev. Lett. **92**, 063902 (2004).
14. G. G. Paulus, F. Grasbon, H. Walther, P. Villoresi, M. Nisoli, S. Stagira, E. Priori, and S. DeSilvestri, "Absolute phase phenomona in photoionization with few-cycle laser pulses," Nature **414**, 182–184 (2001).
15. S. Stagira, G. Sansone, C. Vozzi, and M. Nisoli, "Classical trajectories of molecules exposed to few-optical-cycle light pulses," Phys. Rev. A **73**, 043403 (2006).
16. H. Niikura, D. M. Villeneuve, and P. B. Corkum, "Controlling vibrational wave packets with intense, few-cycle laser pulses," Phys. Rev. A **73**, 021401(R) (2006).
17. P. J. Ho and J. H. Eberly, "Classical effects of laser pulse duration on strong-field double ionization," Phys. Rev. Lett. **95**, 193002 (2005).
18. H. Ihee, V. A. Lobastov, U. M. Gomez, B. M. Goodson, R. Srinivasan, C.-Y. Ruan, and A. H. Zewail, "Direct imaging of transient molecular structures with ultrafast diffraction," Science **291**, 458–462 (2001).
19. A. M. Lindenberg, J. Larsson, K. Sokolowski-Tinten, K. J. Gaffney, C. Blome, O. Synnergren, J. Sheppard, C. Caleman, A. G. MacPhee, D. Weinstein, D. P. Lowney, T. K. Allison, T. Matthews, R. W. Falcone, A. L. Cavalieri, D. M. Fritz, S. H. Lee, P. H. Bucksbaum, D. A. Reis, J. Rudati, P. H. Fuoss, C. C. Kao, D. P. Siddons, R. Pahl, J. Als-Nielsen, S. Duesterer, R. Ischebeck, H. Schlarb, H. Schulte-Schrepping, T. Tschentscher, J. Schneider, D. von der Linde, O. Hignette, F. Sette, H. N. Chapman, R. W. Lee, T. N. Hansen, S. Techert, J. S. Wark, M. Bergh, G. Huldt, D. van der Spoel, N. Timneanu, J. Hajdu, R. A. Akre, E. Bong, P. Krejcik, J. Arthur, S. Brennan, K. Luening, and J. B. Hastings, "Atomic-scale visualization of inertial dynamics," Science **308**, 392–395 (2005).
20. M. Drescher, M. Hentschel, R. Kienberger, G. Tempea, C. Spielmann, G. A. Reider, P. B. Corkum, and F. Krausz, "X-ray pulses approaching the attosecond frontier," Science **291**, 1923–1927 (2001).
21. P. M. Paul, E. S. Toma, P. Breger, G. Mullot, F. Auge, P. Balcou, H. G. Muller, and P. Agostini, "Observation of a train of attosecond pulses from high harmonic generation," Science **292**, 1689–1692 (2001).
22. M. Hentschel, R. Kienberger, C. Spielmann, G. A. Reider, N. Milosevic, T. Brabec, P. Corkum, U. Heinzmann, M. Drescher, and F. Krausz, "Attosecond metrology," Nature **414**, 509–513 (2001).
23. P. Johnsson, R. Lopez-Martens, S. Kazamias, J. Mauritsson, C. Valentin, T. Remetter, K. Varju, M. B. Gaarde, Y. Mairesse, H. Wabnitz, P. Salieres, P. Balcou, K. J. Schafer, and A. L'Huillier, "Attosecond electron wave packet dynamics in strong laser fields," Phys. Rev. Lett. **95**, 013001 (2005).
24. S. X. Hu and L. A. Collins, "Attosecond pump probe: exploring ultrafast electron motion inside an atom," Phys. Rev. Lett. **96**, 073004 (2006).
25. M. Wickenhauser, X. M. Tong, and C. D. Lin, "Laser-induced substructures in above-threshold-ionization spectra from intense few-cycle laser pulses," Phys. Rev. A **73**, 011401(R) (2006).
26. S. Sepke and D. Umstadter, "Analytical solutions for the electromagnetic fields of tightly focused laser beams of arbitrary pulse length," Opt. Lett. **31**, 2589–2591 (2006).
27. S. Banerjee, S. Sepke, R. Shah, A. Valenzuela, A. Maksimchuk, and D. Umstadter, "Optical deflection and temporal characterization of ultra-fast laser produced electron beams," Phys. Rev. Lett. **95**, 035004 (2005).
28. B. Quesnel and P. Mora, "Theory and simulation of the interaction of ultraintense laser pulses with electrons in vacuum," Phys. Rev. E **58**, 3719–3732 (1998).
29. A. Maltsev and T. Ditmire, "Above threshold ionization and in tightly focused, strongly relativistic laser fields," Phys. Rev. Lett. **90**, 053002 (2003).
30. H. Hora, *Laser Plasma Physics* (SPIE Press, 2000).
31. L. Cicchitelli, H. Hora, and R. Postle, "Longitudinal field components for laser beams in vacuum," Phys. Rev. A **41**, 3727–3732 (1990).
32. H. Hora, M. Hoelss, W. Scheid, J. W. Wang, Y. K. Ho, F. Osman, and R. Castillo, "Principle of high accuracy for the nonlinear theory of the acceleration of electrons in a vacuum by lasers at relativistic intensities," Laser Part. Beams **18**, 135–144 (2002).
33. S. Weber, G. Riazuelo, P. Michel, R. Loubere, F. Walraet, V. T. Tikhonchuk, V. Malka, J. Ovadia, and G. Bonnaud, "Modeling of laser-plasma interaction on hydrodynamic scales: physics development and comparison with experiments," Laser Part. Beams **22**, 189–195 (2004).
34. A. E. Siegman, *Lasers* (University Science, 1986).
35. M. Lax, W. H. Louisell, and W. B. McKnight, "From Maxwell to paraxial wave optics," Phys. Rev. A **11**, 1365–1370 (1975).
36. L. W. Davis, "Theory of electromagnetic beams," Phys. Rev. A **19**, 1177–1179 (1979).
37. H. Hora, *Physics of Laser Driven Plasmas* (Wiley, 1981).
38. J. P. Barton and D. R. Alexander, "Fifth order corrected

electromagnetic field components for a fundamental Gaussian beam," J. Appl. Phys. **66**, 2800–2802 (1989).
39. J. X. Wang, W. Sheid, M. Hoelss, and Y. K. Ho, "Fifth-order corrected field descriptions of the Hermite–Gaussian (0, 0) and (0, 1) mode laser beam," Phys. Rev. E **64**, 066612 (2001).
40. P. X. Wang and J. X. Wang, "Classical field description for ultrashort tightly-focused laser pulses," Appl. Phys. Lett. **81**, 4473–4475 (2002).
41. J. F. Hua, Y. K. Ho, Y. Z. Lin, Z. Chen, Y. J. Xie, S. Y. Zhang, Z. Yan, and J. J. Xu, "High-order corrected fields of ultrashort, tightly-focused laser pulses," Appl. Phys. Lett. **85**, 3705–3707 (2004).
42. G. P. Agrawal and D. N. Pattanayak, "Gaussian beam propagation: beyond the paraxial approximation," J. Opt. Soc. Am. **69**, 575–578 (1979).
43. P. Varga and P. Török, "The Gaussian wave solution of Maxwell's equations and the validity of scalar wave approximation," Opt. Commun. **152**, 108–118 (1998).
44. S. Sepke and D. Umstadter, "Exact analytical solution for the vector electromagnetic field of Gaussian, flattened Gaussian, and annular Gaussian laser modes," Opt. Lett. **31**, 1447–1449 (2006).
45. S. Sepke and D. Umstadter, "Analytical solutions for the electromagnetic fields of flattened and annular Gaussian laser modes. I. Small *F*-number laser focusing," J. Opt. Soc. Am. B **23**, 2157–2165 (2006).
46. S. Sepke and D. Umstadter, "Analytical solutions for the electromagnetic fields of flattened and annular Gaussian laser modes. II. Large *F*-number laser focusing," J. Opt. Soc. Am. B **23**, 2166–2173 (2006).
47. M. Abramowitz and I. A. Stegun, eds., *Handbook of Mathematical Functions*, 12th ed. (Dover, 1972).
48. R. Haberman, *Elementary Applied Partial Differential Equations with Fourier Series and Boundary Value Problems*, 3rd ed. (Prentice-Hall, 1997).
49. A. Ludu and R. F. O'Connell, "Laplace transform of spherical Bessel functions," Phys. Scr. **65**, 369–372 (2002).